ACS Catalysis

Research Article

pubs.acs.org/acscatalysis

Deactivation Behavior of Co/TiO_2 Catalysts during Fischer–Tropsch Synthesis

Thomas O. Eschemann* and Krijn P. de Jong*

Inorganic Chemistry and Catalysis, Debye Institute for Nanomaterial Science, Utrecht University, P.O. Box 80083, 3508 TB Utrecht, The Netherlands

Supporting Information

ABSTRACT: Here we report on the preparation of Co/TiO_2 catalysts (8 and 16 wt % Co) using deposition precipitation by ammonia evaporation (DPA) and incipient wetness impregnation with subsequent static drying (IWI-S) and fluidized bed drying (IWI-F). Although the initial cobalt oxide dispersions were similar for catalysts with the same metal loading, the distribution of the nanoparticles over the support surface was found to increase in the order IWI-S < IWI-F < DPA. Initial activities during Fischer–Tropsch synthesis at 493 K, 20 bar were found to increase in the same order, whereas the C_{5+} selectivities were significantly higher for catalysts prepared by DPA. After 200 h of Fischer–Tropsch synthesis at 35% X_{CO}, all systems studied had lost about 20% of their initial activity, which could be completely attributed to a loss in active metal surface area, as shown by TEM histogram analysis. Deactivation constants determined using second-order deactivation kinetics were in the same order of magnitude as for Co/SiO_2 catalysts studied previously, but surprisingly, they were not affected by the distribution of cobalt. Catalysts tested at higher X_{CO} were found to show significantly faster deactivation, which could also be attributed to cobalt particle growth.

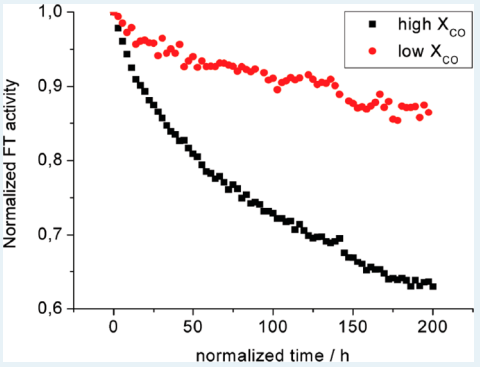

KEYWORDS: *Fischer–Tropsch, cobalt, titania, deactivation, particle growth*

INTRODUCTION

The Fischer–Tropsch reaction involves the catalytic conversion of synthesis gas into higher hydrocarbons and is a promising route to ultraclean fuels, lubricants, and chemicals. Different feedstocks can be used for the generation of the synthesis gas, such as coal, biomass, or natural gas, the latter being most interesting from an economic perspective in the context of stranded natural gas and shale gas.[1−6] Besides the choice of feedstock for synthesis gas generation, investment and operating costs, reactor technology, and oil and gas price development, the performance of the catalyst system is a key factor for the economic viability of Fischer–Tropsch plants.[7,8] Catalyst performance can be divided into three aspects: activity, selectivity, and stability. High activities per unit volume are favored, although mass transfer limitations may occur in industrially used catalyst pellets. More importantly, a high selectivity to heavier hydrocarbons (C_{5+}) is desired. Furthermore, the catalyst should feature a high stability under operating conditions. This criterion is especially important for fixed bed processes, in which exchanging catalysts is a more complex and time-consuming operation compared to slurry bubble column processes.[7−9]

The problem of cobalt Fischer–Tropsch catalyst deactivation has been reviewed extensively.[10,11] The deactivation mechanisms discussed in literature include poisoning, carbon effects (e.g., coking, carbidization, and fouling), reoxidation, formation of cobalt-support compounds, cobalt surface rearrangement, mechanical disaggregation, and loss of cobalt surface area by particle growth. Bulk oxidation has been found to be unlikely under typical Fischer–Tropsch process conditions, although surface oxidation at high water partial pressures may be possible.[11,12] Poisoning effects are highly dependent on the utilized feedstock for synthesis gas generation and the applied gas purification technology, making it an extremely complex phenomenon to be studied at laboratory scale.[13] Cobalt particle growth, however, has been a topic that has received attention both from industrial and academic side and has been identified to be a key factor in catalyst deactivation.[10,11,14−17]

Because the Hüttig temperature of cobalt (526 K) is close to the operating conditions of the low temperature Fischer–Tropsch synthesis (typically 473−513 K),[18] particle growth can occur either via particle migration and coalescence or via Ostwald ripening.[19] Both the partial pressure of water and the formation of cobalt carbonyl species can play a role in the extent of the competing particle growth mechanisms.[16,19,20] Beside the operating conditions, the structure of the catalyst might play an important role for its stability against deactivation by particle growth. It has previously been shown for different catalytic systems that an enhanced spacing of supported nanoparticles can have a distinct positive effect on the catalyst stability against

Received: February 9, 2015
Revised: March 22, 2015
Published: April 24, 2015

DOI: 10.1021/acscatal.5b00268
ACS Catal. 2015, 5, 3181−3188

particle growth.[21−23] For the synthesis of catalysts with well-distributed supported nanoparticles, different techniques can be applied, such as improved drying and heat treatment protocols,[21,24] including freeze-drying[23] for impregnated catalysts, or using deposition precipitation as an alternative catalyst preparation method.[25−27]

We have previously demonstrated that in the synthesis of Co/TiO_2 catalysts, the use of deposition precipitation via ammonia evaporation (DPA)[28] leads to an improved distribution of cobalt over the support material at similar cobalt particle sizes compared to a standard incipient wetness impregnation protocol with subsequent static drying (IWI-S). The more uniform distribution of cobalt was shown to lead to less particle growth during reduction of the catalyst and higher activities in the Fischer−Tropsch reaction under industrial conditions. It was also shown that the catalysts prepared by deposition precipitation feature distinctly higher selectivities to heavy hydrocarbons for a broad metal loading range (4−24 wt % Co), which is important for industrial applications.[25]

Here we report on the deactivation behavior for the first 200 h on stream under industrially relevant conditions of the catalytic systems mentioned above. Furthermore, we apply incipient wetness impregnation with subsequent fluidized bed drying (IWI-F) in order to obtain an improved cobalt distribution without observing the selectivity effects present in catalysts prepared via deposition precipitation. We study the influence of the preparation methods on the cobalt distribution using transmission electron microscopy. The relative loss of activity of the catalysts at comparable CO conversion levels is discussed and the average cobalt particle sizes before and after the catalytic testing experiments are measured using transmission electron microscopy in order to determine the turnover frequencies (TOF) of the catalysts at the start and at the end of the catalytic tests. These values can be used in order to draw conclusions on the main reasons for catalyst deactivation on the time scale of the experiments carried out.

MATERIALS AND METHODS

Catalyst Synthesis. Two methods were applied for the preparation of Co/TiO_2 catalysts by incipient wetness impregnation (IWI). TiO_2 (Aeroxide P25, Evonik Degussa, pore volume 0.3 mL/g, BET surface area 50 m^2/g, 70% anatase, 30% rutile) was presieved to particles of 75−150 μm and dried under vacuum (50 mbar), before the support material was impregnated with an aqueous solution of $Co(NO_3)_2{\cdot}6H_2O$ (Acros, p.a.). The material was then dried in an oven under static air at 333 K overnight. After that, the catalyst was heat treated at 623 K (2 h, ramp 2 K/min) in a fluidized bed under a flow of N_2. These catalysts are labeled IWI-XXS, XX being the weight percentage of Co, assuming Co to be in the form of Co_3O_4. Alternatively, the material was dried in a fluidized bed under a flow of N_2 at 353 K, before the heat treatment was carried out at 623 K (2 h, ramp 2 K/min) in a fluidized bed under a flow of N_2. These catalysts are labeled IWI-XXF. It should be noted that metal loadings of 8 wt % Co (assuming Co to be in the form of Co_3O_4) were achieved with a single impregnation, while for catalysts with 16 wt % Co a second impregnation cycle was carried out after the heat treatment of the sample after the first impregnation.

The preparation method[28] of Co/TiO_2 catalysts by ammonia evaporation deposition precipitation was described before.[25] Initially, 24.75 g of $CoCO_3$ (Acros, p.a.) was dissolved in 255.6 g of 25 wt % ammonia solution (Merck, p.a.); subsequently, 24.75 g of $(NH_4)_2CO_3$ (Acros, p.a.) was added, and the mixture was diluted to give a total of 500 mL. Eight milliliters of this stock solution was mixed with 70 mL of 9 wt % ammonia solution and used to suspend an appropriate amount of TiO_2 powder (0.5−4.0 g) in a PTFE round-bottom flask. The flask was equipped with a reflux cooler and the suspension was stirred and heated to 373 K for 3 h while air was not excluded. After cooling to ambient temperature, the material was filtered off, washed thoroughly with water, and dried at 333 K overnight. The obtained filter cake was crushed and sieved to 75−150 μm and then heat-treated in a flow of N_2 at 673 K (4 h, ramp 5 K/min). The catalysts are labeled DPA-XX.

Catalyst Characterization. X-ray powder diffraction (XRD) was performed on a Bruker D2 Phaser with a Co Kα (λ = 1.789 Å) source. Co_3O_4 crystallite size estimation was performed using the Co_3O_4 peak at 37° 2Q with an automatic calculation routine in DiffracEvaluation V2.0 software by Bruker, which is based on the Debye−Scherrer-equation.

For Transmission Electron Microscopy (TEM), the heat-treated catalysts were ground with a mortar, suspended in ethanol using an ultrasonic bath and dropped onto a copper grid with holey carbon film. Spent catalysts were prepared in the same way. The samples were analyzed using a Tecnai T10 or Tecnai T12 microscope, with electron beam voltage of 100 kV or 120 kV, respectively. Equivalent cobalt particle sizes are calculated from average Co_3O_4 particle sizes based on analysis of typically 200 particles by using the relation d(Co) = d(Co_3O_4) * 0.75. Spent catalysts showed metallic cobalt particles covered with a thin wax layer, and therefore, no correction factor was used.

Catalytic Testing. Fischer−Tropsch synthesis was carried out in a 16 reactor catalytic setup (Flowrence, Avantium). The catalysts were diluted with SiC (200 μm) to arrive at the same amount of Co in every reactor, giving a catalyst bed volume of 200 μL. The catalysts were dried in a flow of He for 2 h and then reduced in situ in a flow of H_2/He (1:3 v/v) at 623 K (8 h, ramp 1 K/min). Subsequently, the reactors were cooled to 453 K and pressurized to 20 bar under a flow of H_2. After switching to H_2/CO/He (190:95:15 v/v, GHSV 3450−5850 h^{-1}) the temperature was increased to 493 K (ramp 1 K/min). At the end of the experiment, most of the products remaining in the catalyst bed were removed under a flow of H_2 at 473 K, before the setup was cooled to room temperature under a flow of He. The products were analyzed using online gas chromatography (Agilent 7890A). The permanent gases were separated on a Shincarbon column and quantified against He as an internal standard using a TCD detector. CO conversions were calculated as

$$X_{CO} = (\mathrm{mol}_{CO\,in} - \mathrm{mol}_{CO\,out})/\mathrm{mol}_{CO\,in} \quad (1)$$

Hydrocarbons (C1−C9) were separated on a PPQ column, detected using an FID detector and quantified against the TCD signal of the internal standard He, making use of the corresponding areas A, the He flow f and the response factor RF.

$$Y_{C_X} = A_{FID}(C_X)/A_{TCD}(He)*RF(C_X/He)/f(He) \quad (2)$$

Selectivities to the lower hydrocarbon fractions S_{C_X} were calculated from converted CO and the corresponding yields as

$$S_{C_X} = Y_{C_X}/(\mathrm{mol}_{CO\,in} - \mathrm{mol}_{CO\,out}) \quad (3)$$

The selectivities to products with 5 and more carbon atoms are calculated from the yields to lower hydrocarbons as

$$S_{C5+} = 1 - S_{C1-C4} \quad (4)$$

DOI: 10.1021/acscatal.5b00268
ACS Catal. 2015, 5, 3181−3188

CO conversion levels during the experiments were between 25 and 35%. Activities are reported as cobalt time yields (CTY, $mol_{CO}/(g_{Co}\cdot s)$) and weight time yields (WTY, $mol_{CO}/(g_{Cat}\cdot s)$). In order to analyze the deactivation of the catalysts, the activities, a, were determined by assuming first-order kinetics in hydrogen according to

$$a = \mathrm{GHSV}^{*}\log(1 - X_{H_2}) \quad (5)$$

These activities were then normalized ($a_{norm} = a/a_{initial}$) as done previously. Although the activity loss in the first 24 h is assigned a.o. to pore filling of the catalyst with FT liquid products, the data point for normalization ($t = 0$, $a_{initial}$) is selected 24 h after reaching FTS conditions (Figure 1). The data

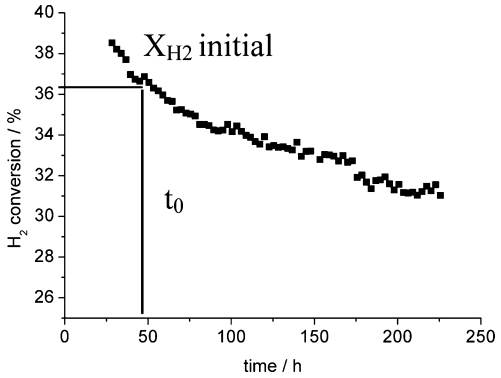

Figure 1. Normalization for deactivation curve of DPA08 during FTS at 493 K, 20 bar, H_2/CO 2.0 v/v.

was then fitted according to a linearized form of second order deactivation kinetics as demonstrated previously for the quantification of deactivation data for Co/SiO_2 Fischer–Tropsch catalysts[22] and $CuZn/SiO_2$ catalysts for methanol synthesis.[21]

$$1/(a_{norm}(t)) = k_d{}^{*}t + 1 \quad (6)$$

RESULTS AND DISCUSSION

The results for the Co_3O_4 particle size of the catalysts obtained after heat treatment determined from XRD and TEM (Table 1)

Table 1. Co_3O_4 Crystallite Sizes Determined from Scherrer Analysis of the XRD peak at 37° 2Θ and Surface-Average Co_3O_4 Particle Sizes Determined by TEM

catalyst	IWI08S	IWI16S	IWI08F	IWI16F	DPA08	DPA16
XRD Co_3O_4 crystallite size \ nm	8.4	12	6.9	12	8.5	13
TEM Co_3O_4 particle size \ nm	8.2	11	7.8	10	7.0	11

showed that for comparable metal loadings similar particle sizes were obtained for all applied preparation techniques. As expected and in accordance with results reported previously,[25] the average particle sizes were found to be larger for the catalysts with higher metal loadings. TEM revealed that the supported Co_3O_4 particles were strongly clustered for the catalysts dried in static air. Distinctly less clustering was obtained for catalysts dried under a flow of nitrogen and uniform distributions were found for the catalysts prepared by deposition precipitation.(Figure 2) These

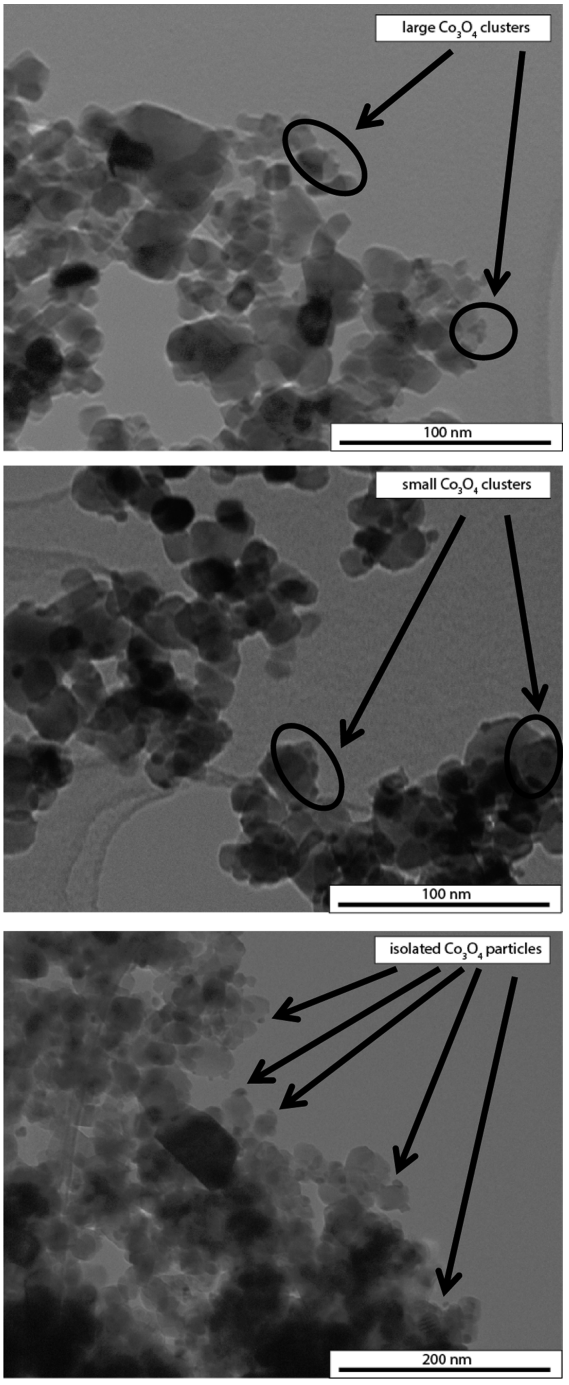

Figure 2. Representative TEM figures of Co_3O_4/TiO_2 catalysts (8 wt % Co) showing larger numbers of agglomerated Co_3O_4 particles for IWI-S catalysts (top), smaller numbers of agglomerated Co_3O_4 clusters for IWI-F catalysts (middle), and more uniformly distributed isolated supported Co_3O_4 particles for DPA catalysts.

results are in accordance with results reported previously indicating improved distributions of supported metal nanoparticles for fluidized bed drying[24] and deposition precipitation.[25]

The performance of the catalysts was studied at 20 bar and 493 K and at similar CO conversion levels (Table 2). For low and high metal loadings, the lowest cobalt time yields (CTY) were obtained for catalysts prepared by incipient wetness impregnation with subsequent static drying. Higher activities were found

DOI: 10.1021/acscatal.5b00268
ACS Catal. 2015, 5, 3181–3188

Table 2. Results for Fischer–Tropsch Synthesis at 493 K, 20 bar, H_2/CO 2.0 v/v[a]

catalyst	X_{CO} initial (%)	X_{CO} final (%)	CTY initial (10^{-5} $mol_{CO}/(g_{Co}*s)$)	CTY final (10^{-5} $mol_{CO}/(g_{Co}*s)$)	S_{CH_4} (%)	$S_{C_{5+}}$ (%)
IWI08S	35.3	30.6	7.0	6.2	8	85
IWI16S	36.2	28.7	8.3	6.8	10	83
IWI08F	36.5	29.2	10.4	8.2	8	85
IWI16F	36.4	30.2	9.1	7.4	9	83
DPA08	36.1	30.7	11.2	9.0	6	90
DPA16	29.0	26.1	10.1	9.0	6	90

[a]Initial data for X_{CO}, S_{CH_4}, and $S_{C_{5+}}$ and CTY after reaching synthesis conditions, final data after 200 h.

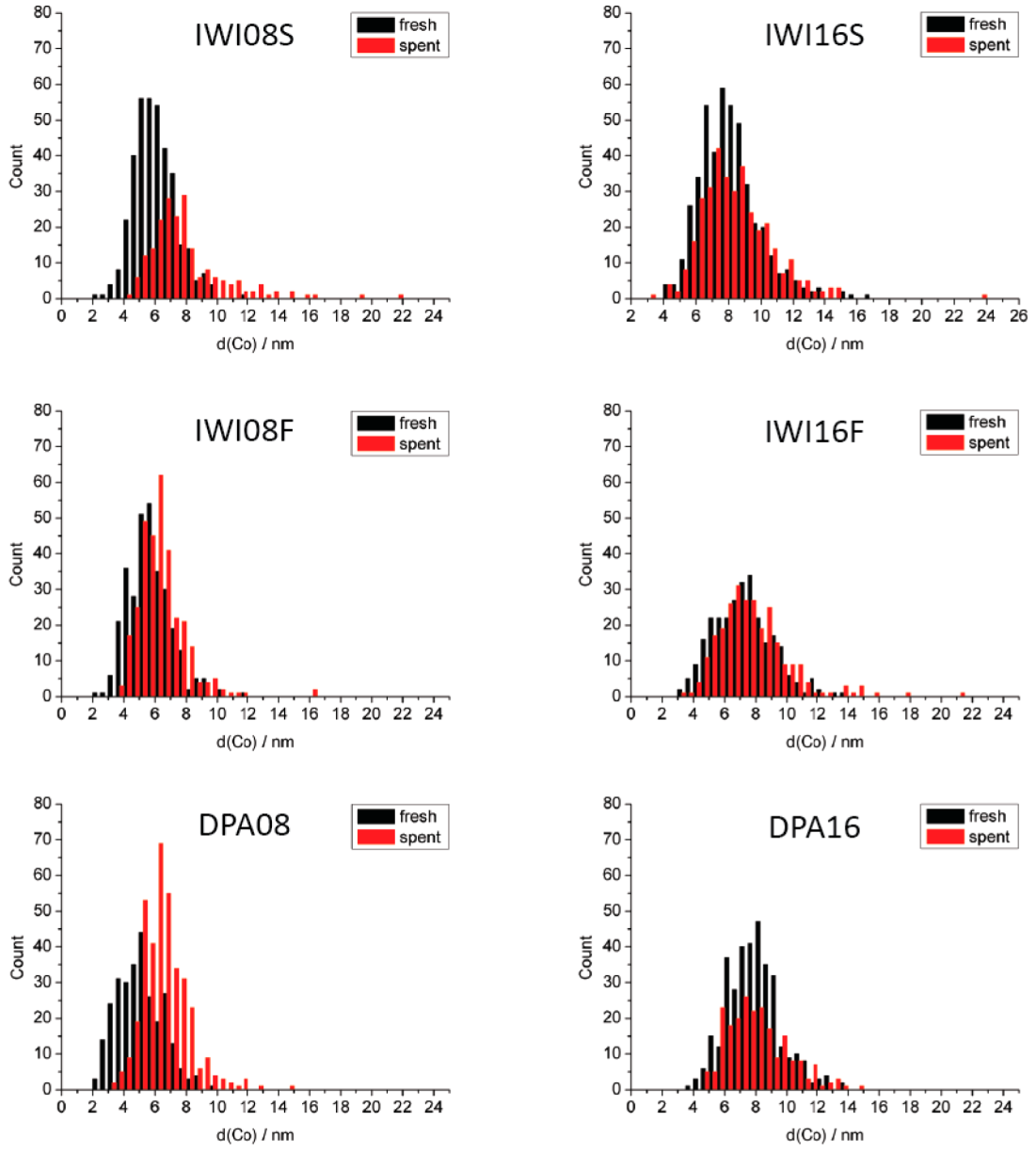

Figure 3. Histograms for TEM cobalt particle size analysis of fresh and spent catalysts.

for catalysts prepared by incipient wetness impregnation with subsequent fluidized bed drying, and even higher activities were determined for the catalysts prepared by deposition precipitation. These values correlate with the degree of cobalt oxide clustering prior to reduction and can be rationalized by a stronger tendency for particle growth during reduction in the case of the clustered catalysts as reported previously.[25] Although for the static drying method, a higher cobalt time yield was found for higher metal loading, the opposite was the case for the catalysts prepared by fluidized bed drying. The C_{5+}-selectivities of all impregnated catalysts were similar between 83 and 85 wt %, whereas the results showed distinctly lower methane selectivities and higher C_{5+}-selectivities of 90 wt % for the DPA catalysts at very similar conversion levels, which has been reported before.[25]

In order to obtain information on the cause of the activity loss of the catalysts, particle size analysis of the fresh and spent

DOI: 10.1021/acscatal.5b00268
ACS Catal. 2015, 5, 3181–3188

Table 3. Turnover Frequencies (TOF) during Fischer–Tropsch Synthesis at 493 K, 20 bar, H_2/CO 2.0 v/v[a]

catalyst	d_{Co} fresh (nm)	d_{Co} spent (nm)	TOF initial (10^{-3} s^{-1})	TOF final (10^{-3} s^{-1})
IWI08S	6.1	7.9	24	24
IWI16S	8.3	8.5	39	34
IWI08F	5.7	6.4	33	30
IWI16F	7.3	7.8	37	33
DPA08	5.2	6.6	33	34
DPA16	8.0	8.1	43	37

[a]Initial X_{CO} 35% for the catalysts in the beginning of the catalytic testing experiment and after 200 h based on TEM surface average particle sizes of the fresh and spent catalysts.

Table 4. Fitting of Deactivation Curves during Fischer–Tropsch Synthesis at 493 K, 20 bar, H_2/CO 2.0 v/v[a]

catalyst	k_d (10^{-4} h^{-1})	R^2	CTY_{final}/ $CTY_{initial}$
IWI08S	5.9	0.99	0.89
IWI16S	11.1	0.99	0.82
IWI08F	12.8	0.99	0.79
IWI16F	11.5	0.99	0.81
DPA08	13.4	0.99	0.80
DPA16	10.8	0.99	0.89

[a]Fitting is according to $1/(a_{norm}(t)) = k_d * t + 1$.

catalysts was carried out using electron microscopy (Figure 3, Table 3). The results show that all catalysts with low cobalt loading show a significant extent of particle growth. For IWI08S, this can be rationalized by the short interparticle distances, whereas for IWI08F and DPA08, the low initial average particle sizes may be a driving factor for particle growth. Smaller increases of particle sizes were found for the catalysts with higher metal loadings, presumably due to the higher initial particle sizes.

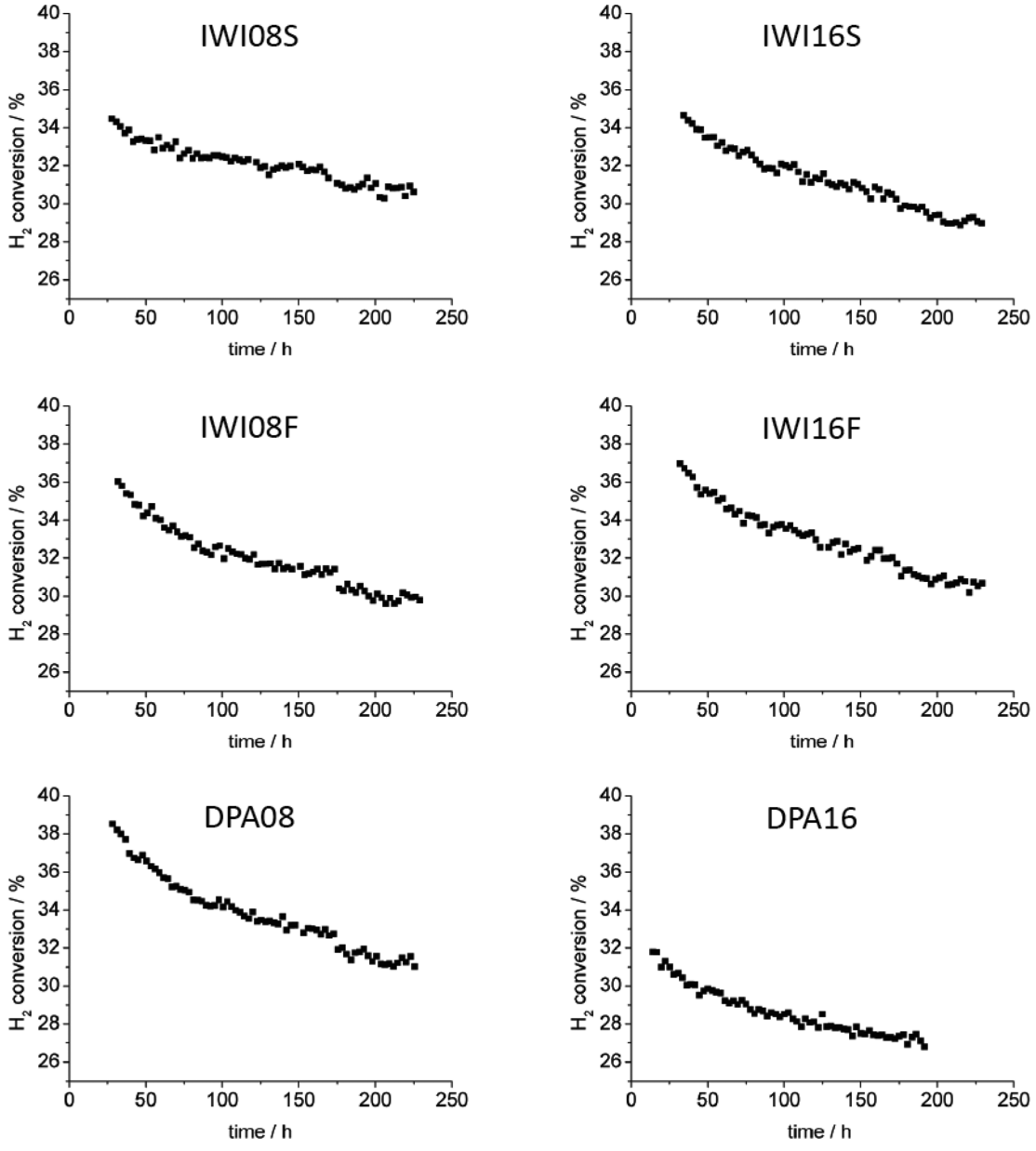

Figure 4. H_2 conversion curves during Fischer–Tropsch synthesis at 493 K, 20 bar, H_2/CO 2.0 v/v for catalysts tested at initial X_{CO} of 35%.

DOI: 10.1021/acscatal.5b00268
ACS Catal. 2015, 5, 3181–3188

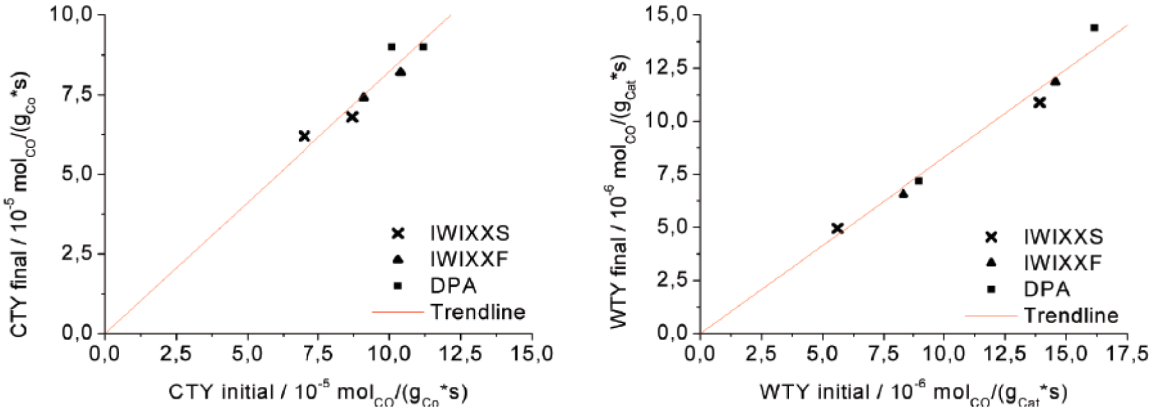

Figure 5. Final (after 200 h) against initial CTY and WTY during Fischer–Tropsch synthesis at 493 K, 20 bar, H_2/CO 2.0 v/v for all catalysts studied at initial X_{CO} 35%. Linear fit with zero intercept; the slopes of the lines are 0.82 and 0.83 respectively.

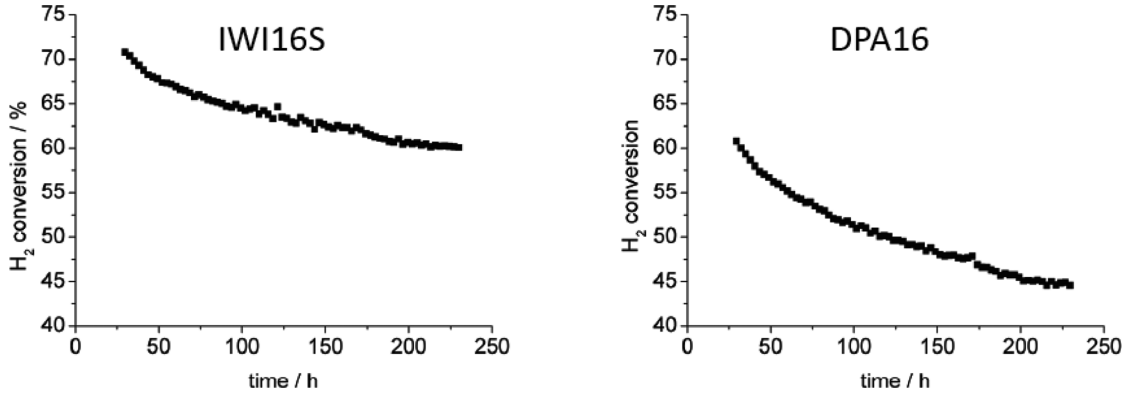

Figure 6. H_2 conversion curves during Fischer–Tropsch synthesis at 493 K, 20 bar, H_2/CO 2.0 v/v for catalysts tested at higher conversions.

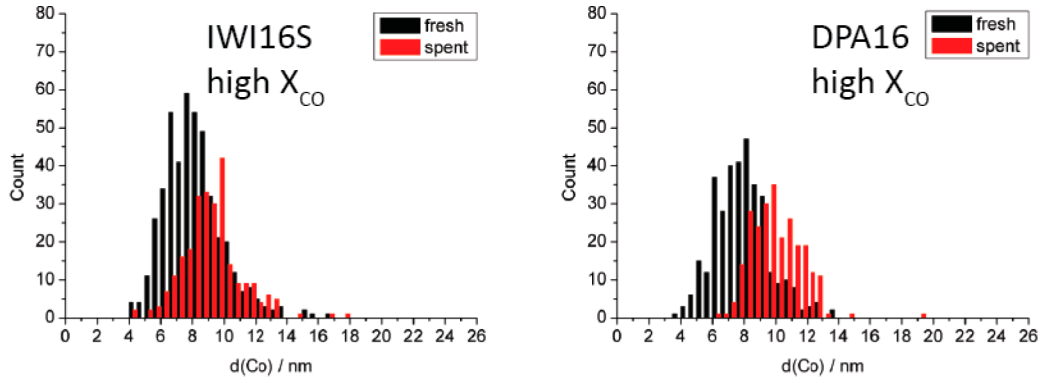

Figure 7. Histograms for TEM cobalt particle size analysis of fresh and spent catalysts tested at high X_{CO}.

Table 5. Turnover Frequencies (TOF) during Fischer–Tropsch Synthesis at 493 K, 20 bar, H_2CO 2.0 v/v, GHSV 3450–5850 h^{-1}[a]

catalyst	X_{CO} initial (%)	d_{Co} fresh (nm)	d_{Co} spent (nm)	TOF initial (10^{-3} s^{-1})	TOF final (10^{-3} s^{-1})
IWI16S	36.2	8.3	8.5	39	34
IWI16S	70.4	8.3	9.4	39	42
DPA16	29.0	8.0	8.1	43	37
DPA16	61.4	8.0	10.1	52	52

[a]Different initial X_{CO} for the catalysts in the beginning of the catalytic testing experiment and after 200 h based on TEM surface average particle sizes of the fresh and spent catalysts.

Table 6. Fitting of Deactivation Curves during Fischer–Tropsch Synthesis at 493 K, 20 bar, H_2/CO 2.0 v/v, GHSV 3450–5850 h^{-1}[a]

catalyst	X_{CO} initial (%)	k_d (10^{-4} h^{-1})	R^2	CTY_{final}/ $CTY_{initial}$
IWI16S	36.2	11.1	0.99	0.82
IWI16S	70.4	15.1	0.99	0.78
DPA16	29.0	10.8	0.99	0.89
DPA16	61.4	24.7	0.99	0.72

[a]Fitting is according to $1/(a_{norm}(t)) = k_d * t + 1$.

Calculations of turnover frequencies for the beginning and for the end of the catalytic experiment were carried out on the basis of the surface average TEM particle sizes (Table 3). The results

DOI: 10.1021/acscatal.5b00268
ACS Catal. 2015, 5, 3181–3188

showed that for the catalysts with low cobalt loadings, no significant change in turnover frequencies were observed, indicating that particle growth explains the loss of activity quantitatively. This is in accordance with the literature listing a loss of active metal surface area the most important factor in the deactivation of cobalt Fischer–Tropsch catalysts during the first hundreds of hours for cobalt Fischer–Tropsch catalysts in general[10,11] and Co/TiO_2 in particular. For catalysts with high metal loadings, somewhat lower turnover frequencies were obtained at the end-of-run. The higher values observed at the start for the highly loaded samples can be attributed to average particle growth during reduction, which was not taken into account in the calculations. Alternatively, the particle size of the fresh catalysts may be underestimated because TEM analysis might not be fully representative although large numbers of particles were measured. The reason for the apparent TOF values reported here being lower than results previously reported[25] relates to the fact that the apparent TOF in this work were calculated from TEM particle sizes rather than from hydrogen chemisorption uptake. Due to SMSI effects the hydrogen chemisorption is expected to be suppressed leading to higher TOF values. Also, in these calculations the degree of reduction is assumed to be high in line with literature,[29] and little variation is expected for catalysts with similar composition, activation, and catalytic testing conditions.

To quantify the deactivation behavior over the time scale of the catalytic experiment, the activity curves based on H_2 conversion (Figure 4) were analyzed and fitted assuming second order deactivation kinetics (Figure S1).

Similar deactivation rates k_d were obtained for all catalysts, with only the values obtained for one impregnated catalyst with subsequent static drying being significantly lower. The relative remaining activity for IWI08S and DPA16 are the highest obtained. The relative remaining activities for all other impregnated catalysts were similar. It should be noted that the ratio of final to initial CTY or WTY for all catalysts is similar and appears to be independent of the catalyst preparation method or the cobalt interparticle spacings of the systems studied in this research (Table 4). The graphs of final CTY/WTY against initial CTY/WTY shows this point even more clearly (Figure 5). The slope of the linear fit for WTY is about 0.8 in line with the loss of about 20% activity for most of the catalysts investigated for 200 h at 35% CO conversion.

Two catalysts were tested at lower GHSV ($1800–3000\ h^{-1}$) in order to study the effect of higher conversions (Figure 6) on the activities and deactivation behavior. TEM histogram analysis of the spent catalysts revealed that average particle growth took place to a higher extent at higher conversions (Figure 7), which can be explained with higher water partial pressures in the reactors.[16] A look at the initial and final TOF frequencies (Table 5) shows that the loss in activity can mostly be attributed to average particle growth. Interestingly, the final turnover frequencies at high CO conversion levels of IWI16S are slightly higher and distinctly higher for DPA16 compared to the values obtained at lower CO conversion levels. This can be explained by the autocatalytic effect of water that has previously been demonstrated to have a positive effect on reaction rates of Co/TiO_2 catalysts.[30]

A look at the deactivation curves of catalysts tested at lower GHSV (Figure 6, Figure S2) showed higher deactivation rate constants for IWI16S and lower remaining activities in the end of the catalytic testing experiment for DPA16 (Table 6). These results indicate that higher water partial pressures enhance deactivation by particle growth as suggested previously.[16]

CONCLUSIONS AND OUTLOOK

The results show that the catalyst preparation method has a strong impact on the cobalt distribution on the titania support material. It was demonstrated that fluidized bed drying leads to more uniform cobalt distributions compared to conventional static drying, while the use of deposition precipitation led to even largely homogeneous cobalt distributions. Results from Fischer–Tropsch synthesis at 493 K and 20 bar revealed higher activities for systems with more uniform distribution of cobalt, which can be rationalized with the higher accessible cobalt surface area during Fischer–Tropsch synthesis. The C_{5+}-selectivity was not found to be affected by differences in cobalt distribution for the impregnated catalysts, but superior selectivities were found for the systems prepared by deposition precipitation, as has been shown earlier.[25] Catalytic testing experiments for 200 h showed that all catalysts lose about 20% of their activity likely due to average particle growth, as was shown by TEM analysis of the fresh and spent catalysts and turnover frequency calculations. Constant turnover frequencies calculated for the catalysts with low metal loadings suggest that the loss in activity can be attributed to a loss of cobalt surface area, which is in accordance with results reported elsewhere.[17] It should be considered that other deactivation factors may also play a role in this study that could not be experimentally observed, such as surface rearrangement, surface oxidation as well as carbon deposition. The deactivation curves for catalysts at similar CO conversion levels showed that the relative loss in activity is comparable for all catalysts studied in this research and that the cobalt distribution over the support surface does not seem to play a crucial role in the particle growth mechanism, unlike previously shown for Co/SiO_2 Fischer–Tropsch catalysts[22] or other catalytic systems.[21] Being a reducible oxide, TiO_2 deserves special attention due to possible SMSI effects that may be partly reversed during Fischer–Tropsch synthesis, especially at higher conversion. For catalysts with similar composition and particle sizes that are activated and tested under the same conditions, such SMSI effects and their impact on the catalytic properties is expected to be comparable, too. The fact that interparticle spacings do not play a significant role for deactivation makes particle migration less likely as a mechanism for particle growth. Catalytic testing of two catalysts at elevated CO conversion levels showed that the deactivation proceeded faster; for example, higher deactivation rate constants and a higher relative activity loss were observed for IWI16S and DPA16. Also in this case, the loss in activity was found to correlate well with the loss of cobalt surface area during Fischer–Tropsch synthesis. In situ X-ray spectroscopy[31] might be able to give more insight into the reasons of deactivation for these catalysts in the future. In order to study the mechanism of particle growth, for example, Ostwald ripening or migration and coalescence and (quasi)-in situ electron microscopy techniques[32] can be applied in order to obtain further insights.

ASSOCIATED CONTENT

Supporting Information

The following file is available free of charge on the ACS Publications website at DOI: 10.1021/acscatal.5b00268.

Fitted data sets for inversed normalized activities as a function of time (PDF)

DOI: 10.1021/acscatal.5b00268
ACS Catal. 2015, 5, 3181–3188

AUTHOR INFORMATION

Corresponding Authors

*E-mail: k.p.dejong@uu.nl.
*E-mail: T.O.Eschemann@uu.nl.

Notes

The authors declare no competing financial interest.

ACKNOWLEDGMENTS

We gratefully acknowledge Shell Global Solutions for financial support. We also thank Johan den Breejen, Heiko Oosterbeek and Sander van Bavel for fruitful discussions and Rien van Zwienen for technical assistance on high pressure catalytic testing. K.P.d.-J. acknowledges support from NWO-TOP, NRSCC, and an ERC Advanced Grant.

REFERENCES

(1) Dry, M. E. J. *J. Chem. Technol. Biotechnol.* **2002**, *77*, 43−50.
(2) Dry, M. E. *Catal. Today* **2002**, *71*, 227−241.
(3) Van Vliet, O. P. R.; Faaij, A. P. C.; Turkenburg, W. C. *Energy Convers. Manage.* **2009**, *50*, 855−876.
(4) Haarlemmer, G.; Boissonnet, G.; Peduzzi, E.; Setier, P.-A. *Energy* **2014**, *66*, 667−676.
(5) Zennaro, R. In *Greener Fischer−Tropsch Processes for Fuels and Feedstocks*; Maitlis, P. M., de Klerk, A., Eds.; Wiley-VCH: New York, 2013; pp 149−169.
(6) Fox, E. B.; Liu, Z.-T. Z.-W.; Liu, Z.-T. Z.-W. *Energy Fuels* **2013**, *27*, 6335−6338.
(7) De Klerk, A.; Li, Y.-W.; Zennaro, R. In *Greener Fischer−Tropsch Processes for Fuels and Feestock*; Maitlis, P. M., de Klerk, A., Eds.; Wiley-VCH: New York, 2013; pp 53−79.
(8) Khodakov, A. Y.; Chu, W.; Fongarland, P. *Chem. Rev.* **2007**, *107*, 1692−1744.
(9) Sie, S. T.; Krishna, R. *Appl. Catal., A* **1999**, *186*, 55−70.
(10) Tsakoumis, N. E.; Rønning, M.; Borg, Ø.; Rytter, E.; Holmen, A. *Catal. Today* **2010**, *154*, 162−182.
(11) Saib, A. M.; Moodley, D. J.; Ciobîcă, I. M.; Hauman, M. M.; Sigwebela, B. H.; Weststrate, C. J.; Niemantsverdriet, J. W.; van de Loosdrecht, J. *Catal. Today* **2010**, *154*, 271−282.
(12) Van de Loosdrecht, J.; Balzhinimaev, B.; Dalmon, J.-A.; Niemantsverdriet, J. W.; Tsybulya, S. V.; Saib, A. M.; van Berge, P. J.; Visagie, J. L. *Catal. Today* **2007**, *123*, 293−302.
(13) Aasberg-Petersen, K.; Dybkjær, I.; Ovesen, C. V.; Schjødt, N. C.; Sehested, J.; Thomsen, S. G. J. *J. Nat. Gas Sci. Eng.* **2011**, *3*, 423−459.
(14) Tsakoumis, N. E.; Dehghan-Niri, R.; Rønning, M.; Walmsley, J. C.; Borg, Ø.; Rytter, E.; Holmen, A. *Appl. Catal., A* **2014**, *479*, 59−69.
(15) Argyle, M. D.; Frost, T. S.; Bartholomew, C. H. *Top. Catal.* **2013**, *57*, 415−429.
(16) Bezemer, G. L.; Remans, T. J.; van Bavel, A. P.; Dugulan, A. I. *J. Am. Chem. Soc.* **2010**, *132*, 8540−8541.
(17) Soled, S. L.; Kiss, G.; Kliewer, C.; Baumgartner, J.; El-Malki, E.-M. *Chemistry of Energy and Food*, Proceedings of the ACS National Meeting & Exposition, New Orleans, Louisiana, April 7−11, 2013; American Chemical Society: Washington, DC, 2013.
(18) Moulijn, J. A.; van Diepen, A. E.; Kapteijn, F. *Appl. Catal., A* **2001**, *212*, 3−16.
(19) Davis, B. H. In *Greener Fischer−Tropsch Processes for Fuels and Feestocks*; Maitlis, P. M., de Klerk, A., Eds.; Wiley-VCH: New York, 2013; pp 193−207.
(20) Sadeqzadeh, M.; Chambrey, S.; Piché, S.; Fongarland, P.; Luck, F.; Curulla-Ferré, D.; Schweich, D.; Bousquet, J.; Khodakov, A. Y. *Catal. Today* **2013**, *215*, 52−69.
(21) Prieto, G.; Zečević, J.; Friedrich, H.; de Jong, K. P.; de Jongh, P. E. *Nat. Mater.* **2013**, *12*, 34−39.
(22) Munnik, P.; de Jongh, P. E.; de Jong, K. P. J. *J. Am. Chem. Soc.* **2014**, *136*, 7333−7340.
(23) Eggenhuisen, T. M.; Friedrich, H.; Nudelman, F.; Zečevic, J.; Sommerdijk, N. A. J. M.; Jongh, P. E. de; Jong, K. P. de. *Chem. Mater.* **2013**, *25*, 890−896.
(24) Munnik, P.; Krans, N. A.; de Jongh, P. E.; de Jong, K. P. *ACS Catal.* **2014**, *4*, 3219−3226.
(25) Eschemann, T. O.; Bitter, J. H.; de Jong, K. P. *Catal. Today* **2014**, *228*, 89−95.
(26) De Jong, K. P. In *Synthesis of Solid Catalysts*; de Jong, K. P., Ed.; Wiley-VCH: Weinheim, 2009; pp 111−132.
(27) Van der Lee, M. K.; van Dillen, A. J.; Bitter, J. H.; de Jong, K. P. *J. Am. Chem. Soc.* **2005**, *127*, 13573−13582.
(28) Lok, C. M. Process for preparing cobalt catalysts on titania support. EP1542794, September 25, 2010.
(29) Storsæter, S.; Tøtdal, B.; Walmsley, J. C.; Tanem, B. S.; Holmen, A. *J. Catal.* **2005**, *236*, 139−152.
(30) Iglesia, E. *Appl. Catal., A* **1997**, *161*, 59−78.
(31) Cats, K. H.; Gonzalez-Jimenez, I. D.; Liu, Y.; Nelson, J.; van Campen, D.; Meirer, F.; van der Eerden, A. M. J.; de Groot, F. M. F.; Andrews, J. C.; Weckhuysen, B. M. *Chem. Commun.* **2013**, *49*, 4622−4624.
(32) Hansen, T. W.; Delariva, A. T.; Challa, S. R.; Datye, A. K. *Acc. Chem. Res.* **2013**, *46*, 1720−1730.

DOI: 10.1021/acscatal.5b00268
ACS Catal. 2015, 5, 3181−3188